



Prkdc participates in mitochondrial genome maintenance and prevents Adriamycin-induced nephropathy in mice

Natalia Papeta,¹ Zongyu Zheng,¹ Eric A. Schon,^{2,3} Sonja Brosel,² Mehmet M. Altintas,⁴ Samih H. Nasr,⁵ Jochen Reiser,⁴ Vivette D. D'Agati,⁵ and Ali G. Gharavi¹

¹Department of Medicine, ²Department of Genetics and Development, and ³Department of Neurology, Columbia University College of Physicians and Surgeons, New York, New York, USA. ⁴Department of Medicine, Leonard Miller School of Medicine, University of Miami, Miami, USA.

⁵Department of Pathology, Columbia University College of Physicians and Surgeons, New York, New York, USA.

Adriamycin (ADR) is a commonly used chemotherapeutic agent that also produces significant tissue damage. Mutations to mitochondrial DNA (mtDNA) and reductions in mtDNA copy number have been identified as contributors to ADR-induced injury. ADR nephropathy only occurs among specific mouse inbred strains, and this selective susceptibility to kidney injury maps as a recessive trait to chromosome 16A1-B1. Here, we found that sensitivity to ADR nephropathy in mice was produced by a mutation in the *Prkdc* gene, which encodes a critical nuclear DNA double-stranded break repair protein. This finding was confirmed in mice with independent *Prkdc* mutations. Overexpression of *Prkdc* in cultured mouse podocytes significantly improved cell survival after ADR treatment. While *Prkdc* protein was not detected in mitochondria, mice with *Prkdc* mutations showed marked mtDNA depletion in renal tissue upon ADR treatment. To determine whether *Prkdc* participates in mtDNA regulation, we tested its genetic interaction with *Mpv17*, which encodes a mitochondrial protein mutated in human mtDNA depletion syndromes (MDDSs). While single mutant mice were asymptomatic, *Prkdc/Mpv17* double-mutant mice developed mtDNA depletion and recapitulated many MDDS and ADR injury phenotypes. These findings implicate mtDNA damage in the development of ADR toxicity and identify *Prkdc* as a MDDS modifier gene and a component of the mitochondrial genome maintenance pathway.

Introduction

Adriamycin (ADR) nephropathy is a classic experimental model of kidney disease, resulting from selective injury to glomerular podocytes, the visceral epithelial cells that maintain the kidney filtration barrier (1–3). Genetic or acquired defects that reduce as little as 10%–20% of podocyte cell mass are sufficient to initiate glomerulosclerosis and nephropathy (4–7). In the ADR nephropathy model, a single dose of ADR produces loss of podocyte foot process architecture and progressive podocyte depletion, resulting in persistent proteinuria, followed by the development of focal segmental glomerulosclerosis and finally, global sclerosis (8). This model is frequently used to unmask susceptibility to glomerulosclerosis in genetically manipulated mice or to test the relevance of specific pathways or interventions in the development of nephropathy (1–3, 8–11). However, interpretation of studies using the ADR nephropathy model is limited by our lack of understanding of the underlying mechanism of injury. Therefore, elucidation of the mechanisms of tissue injury in this trait can provide insight into pathways mediating glomerulosclerosis and a biological context for studies using this model. Moreover, because ADR is a commonly used chemotherapeutic drug, better understanding of ADR nephropathy can also offer insight into mechanisms of ADR tissue toxicity (12).

ADR is an anthracycline antibiotic with pleiotropic cytotoxic effects used for treatment of solid and hematogenous tumors. Proposed mechanisms of ADR-induced tissue damage include introduction of double-stranded DNA breaks (DSBs), lipid peroxidation, inhibition of protease activity, disruption of the cyto-

skeletal and extracellular matrix, and inhibition of the topoisomerase II-mediated religation of the broken DNA strands (13–16). In addition, mutations in mitochondrial DNA (mtDNA) and reduction in mtDNA copy number have been increasingly identified as major contributors to ADR-induced tissue injury: ADR can damage mtDNA directly, by intercalating into mtDNA, or indirectly, by generating ROS, producing mtDNA depletion in the kidney and heart after short-term treatment (17–21). Cardiomyopathy, the most common side effect of ADR therapy in humans, is also associated with mtDNA damage, and interventions that improve mitochondrial biogenesis are protective against cardiac dysfunction (20, 21).

The mitochondrion has its own 16-kb circular genome, which undergoes replication independent of the cell cycle. The mtDNA has more rapid turnover than nuclear DNA in all tissues and is particularly prone to ROS-mediated injury, because it lacks histone coverage and is localized closely to the inner mitochondrial membrane, a major site of ROS production in cells (22, 23). Because the majority of mitochondrial proteins are encoded in the nucleus, coordinated interactions between the nuclear and mitochondrial compartments are required for mtDNA replication or repair (24, 25). The components of this signaling pathway have not been fully elucidated but are likely critical for cell survival, especially for that of postmitotic cells, such as podocytes or cardiomyocytes, which have poor regenerative potential.

Most of the information about regulation of mtDNA is derived from genetics studies of mtDNA depletion syndrome (MDDS), a group of genetic disorders characterized by multiple organ dysfunction due to spontaneous mtDNA depletion (26–28). To date, genes implicated in MDDS involve regulation of mtDNA synthe-

Conflict of interest: The authors have declared that no conflict of interest exists.

Citation for this article: *J Clin Invest.* 2010;120(11):4055–4064. doi:10.1172/JCI43721.



sis or deoxynucleotide production and turnover. Intriguingly, although most MDDS-associated genes are ubiquitously expressed, mutations have variable expressivity, with dysfunction in the liver, muscle, or central nervous system among different patients (28). Moreover, in mice, inactivation of some MDDS genes predominantly manifests as renal damage, which can be severe or indolent (ribonucleotide reductase M2 B [*Rrm2b*] or Mpv17 mitochondrial inner membrane protein [*Mpv17*], respectively; refs. 29, 30) focal segmental glomerulosclerosis. The precise reasons underlying the variability in end-organ complication of MDDS are not known, but these data suggest that there are tissue- and cell-specific thresholds for tolerance of mtDNA damage. Moreover, the occurrence of mtDNA depletion in both ADR nephropathy and MDDS suggests a shared pathogenesis between these traits, indicating that understanding the genetic basis of ADR nephropathy can inform not only about mechanisms of ADR-mediated toxicity but may also clarify pathways mediating mtDNA maintenance.

Mouse laboratory strains demonstrate contrasting susceptibility to ADR nephropathy, allowing application of genetics approaches to elucidate the underlying biology. We had previously performed systematic screening of 15 inbred strains and identified 3 highly susceptible strains (BALB/cJ [BALB], 129S1/SvImJ, and 129X1/SvJ), while other strains (such as C57BL/6J [B6]) were completely resistant (31, 32). We had also shown that this dichotomous susceptibility among inbred strains segregates as a single-gene recessive defect that maps to chromosome 16A1-B1 (31). Because laboratory strains are derived from a limited set of ancestors, this suggested that the shared susceptibility represents inheritance of the same ancestral susceptibility allele. Consistent with this hypothesis, high-resolution mapping of the ADR nephropathy locus defined a risk haplotype that predicted susceptibility to nephrotoxicity and allowed us to reduce the locus to a 1.3-Mb segment, containing 20 genes (32).

Here, we demonstrate that a mutation in the protein kinase, DNA-activated, catalytic polypeptide (*Prkdc*) gene is the underlying cause of susceptibility to ADR nephropathy. To determine whether mtDNA depletion is the likely mechanism of injury, we performed a test of genetic interactions that demonstrated that combined mutations in the *Prkdc* and the *Mpv17* genes resulted in early-onset mtDNA depletion and multiple organ injury, recapitulating many MDDS and ADR injury phenotypes in the absence of ADR. This provides evidence for what we believe to be a novel role for *Prkdc* in the MDDS pathway, implicating a nuclear DNA repair protein in the maintenance of mitochondrial genome.

Results

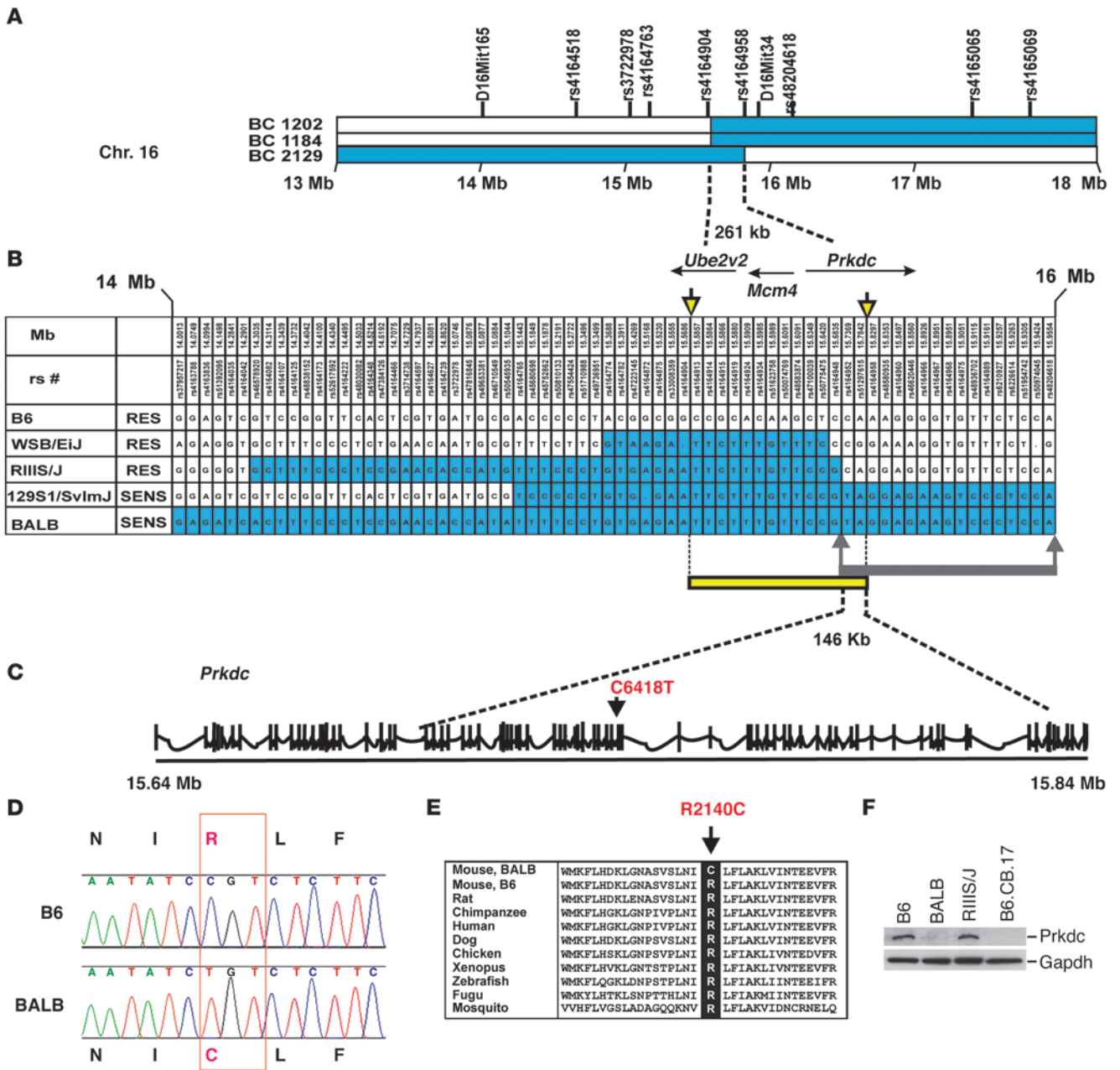
Application of meiotic mapping and haplotype analysis refines the ADR nephropathy susceptibility locus to a mutation in the Prkdc gene. We had previously mapped the murine ADR nephropathy susceptibility locus to a 1.3-Mb segment on chromosome 16A1-B1, containing 20 genes (31, 32). We further refined this map location by meiotic mapping in 1,622 F₂ and backcross progeny between the susceptible BALB and resistant B6 strains. We tested all 68 mice with informative recombinations in this interval for susceptibility to ADR nephropathy, using our standard protocol (31, 32). We identified 4 critical recombinants in affected mice that localized the susceptibility gene to a 261-kb segment flanked by rs4164904 and rs4164958, an interval that contains 3 transcribed genes: *Ube2v2*, *Mcm4*, and *Prkdc* (Figure 1A). To refine this region further, we performed analysis of haplotypes among 48 inbred strains and

identified 1 laboratory strain, RIIS/J, which shows a recombinant haplotype within the minimal meiotic interval. The RIIS/J strain shares a common haplotype with the susceptible BALB strain from 14.31 to 15.73 Mb but transitions to a divergent haplotype distal to rs4164948 (Figure 1B). This 1.42-Mb haplotype, shared between the RIIS/J and BALB strains, also includes an approximately 450-kb segment with a very low polymorphism rate (0.008%) compared with that of the WSB/Eij strain. Given the common origin and limited haplotype structure of laboratory strains (33), the finding of a 1.42-Mb shared segment between the BALB and RIIS/J strains is highly indicative of inheritance by descent from a common founder. Phenotypic screening revealed that RIIS/J, WSB/Eij, and (BALB × RIIS/J) F₁ hybrids are all resistant to ADR nephropathy, thereby localizing the susceptibility allele distal to rs4164948 (Figure 1, B and C). Thus, in combination, the meiotic mapping and haplotype analyses refined the ADR nephropathy locus to a 146-kb interval delimited by rs4164948 and rs4164958, which includes only a part of the *Prkdc* gene, extending from intron 21 through intron 76 (Figure 1C). *Prkdc* was a compelling candidate, because it encodes the catalytic subunit of the DNA-dependent protein kinase, a critical component of the nonhomologous end-joining DNA repair pathway (34), which is particularly important for repair of DSBs in nondividing cells, such as podocytes.

We first sequenced all 56 *Prkdc* exons and flanking introns located within this 146-kb interval and identified a C6418T transition in exon 48 of the gene. This was the only coding variant detected in the critical region, was found among all 3 strains susceptible to ADR nephropathy (BALB, 129S1/SvImJ, and 129X1/SvJ), and was absent in all 17 strains with known resistance, including RIIS/J and WSB/Eij (Fisher's exact test, $P = 0.0009$; refs. 31, 32). The C6418T transition produces a nonconservative substitution, changing codon 2140 of *Prkdc* from CGT (arginine in B6) to TGT (cysteine in BALB; Figure 1D). This R2140C substitution occurs within an amino acid segment that is highly conserved from human to fugu, residing in a larger conserved domain of unknown function (called NUC194; Figure 1E; ref. 35). We next conservatively sequenced all the exons and flanking introns of genes localized within the 261-kb minimal recombinant interval in the resistant B6 and the sensitive BALB strains (*Ube2v2*, *Mcm4*, and *Prkdc*) and found no other coding variants. Further screening of remaining *Prkdc* exons identified another missense variant (A11530G in exon 81), but this variant resides outside the recombinant interval and results in a conservative M3844V substitution. These data indicated that the R2140C variant is most likely the functional mutation underlying susceptibility to ADR nephropathy.

To detect a functional effect of the R2140C variant, we next examined expression of *Prkdc* in the kidney of resistant and susceptible strains. We found no changes in baseline *Prkdc* transcript levels between BALB and B6 strains but detected an 80%–90% reduction in protein abundance in the BALB strain, which was comparable to levels observed in B6.CB17 mice harboring the SCID allele, a spontaneous loss-of-function mutation in *Prkdc* (36). This suggested that the R2140C substitution may affect protein stability and is a loss-of-function mutation, which is also consistent with the recessive transmission of the trait (Figure 1F).

Induction of ADR nephropathy in mice with independent Prkdc mutations confirmed that Prkdc is the ADR nephropathy susceptibility gene. To obtain independent confirmation that a mutation in *Prkdc* is responsible for susceptibility to ADR nephropathy, we tested ADR susceptibility in 2 strains with independent loss-of-function muta-



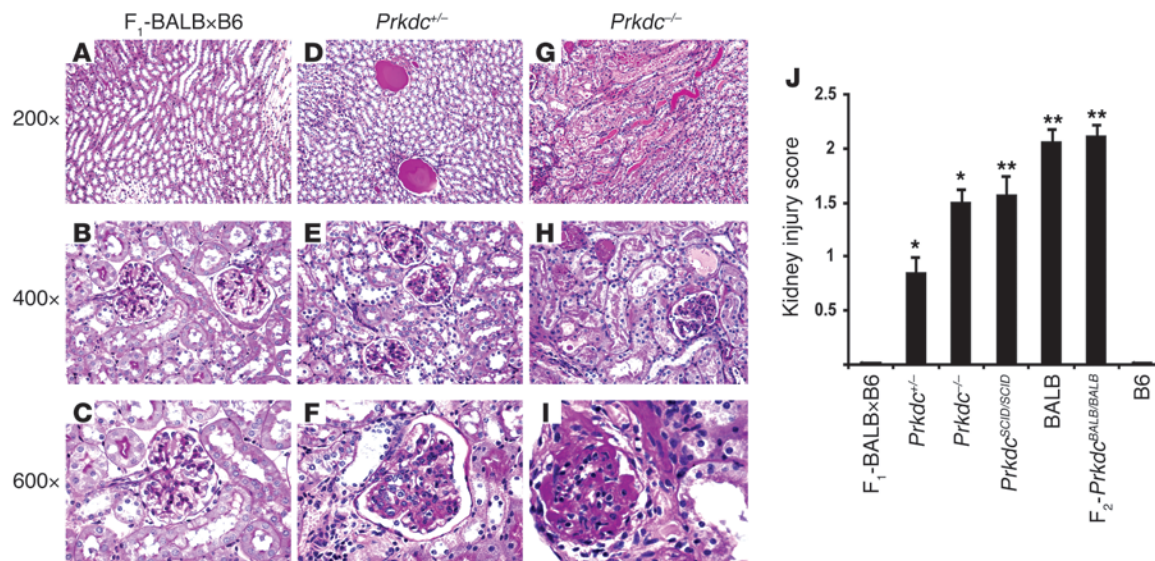


Figure 2

Development of ADR nephropathy in mice with independent mutations in *Prkdc*. (A–C) (BALB × B6) F₁ hybrid mice are resistant to ADR nephropathy. (D–F) *Prkdc*^{+/-} mice develop a mild version of ADR nephropathy with tubulointerstitial dilation, cast formation (D), and glomerular mesangial sclerosis (E and F). (G–I) The *Prkdc*^{-/-} mice develop severe ADR nephropathy, with more abundant casts (G), acute tubular injury (H), and progression to focal global glomerulosclerosis (I). (J) Kidney injury scores in mice with independent *Prkdc* mutations compared with those of resistant B6 and (BALB × B6) F₁ mice. **P* < 0.05, ***P* < 1 × 10⁻⁵, respectively, (*t* test) as compared with B6 and (BALB × B6) F₁ groups. Original magnification: ×200 (top row); ×400 (middle row); ×600 (bottom row).

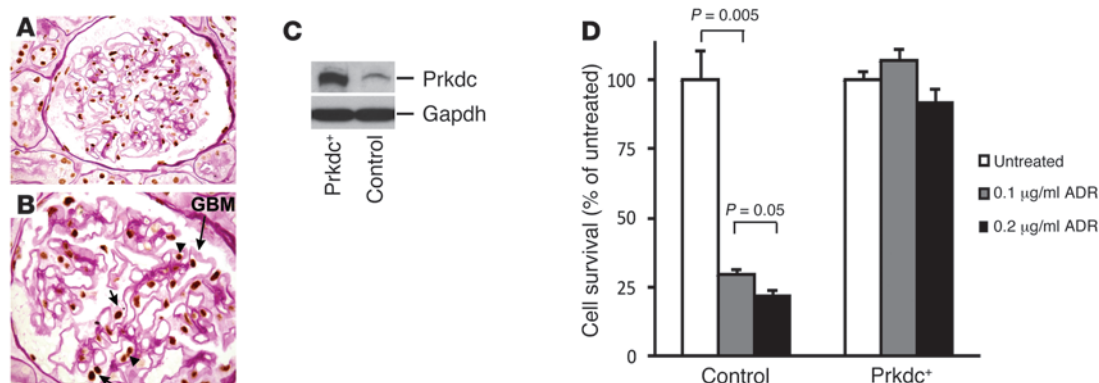
tions in *Prkdc* on the resistant B6 background, the *Prkdc*-KO strain with targeted inactivation of *Prkdc* (37) and the B6.CB17 strain with the spontaneous *Prkdc*^{SCID} allele (36, 38), both resulting in lack of functional Prkdc protein. ADR injection recapitulated the ADR nephropathy phenotype in both strains, with renal histology showing tubular casts, mesangial sclerosis, and FSGS (Figure 2 and Supplemental Figure 2; supplemental material available online with this article; doi:10.1172/JCI43721DS1). The development of ADR-induced nephropathy in strains with independent *Prkdc* mutations on the resistant B6 background provides formal proof that *Prkdc* is the ADR susceptibility gene.

Quantitative comparison of mice with different *Prkdc* alleles demonstrated subtle differences in ADR nephropathy phenotype. Although the BALB, *Prkdc*-KO, and B6.CB17 strains developed similar severity of nephropathy (Figure 2J), the *Prkdc*-KO mice (*Prkdc*^{-/-}; Figure 2, G–I) were most sensitive to ADR administration, which resulted in death by day 7–8 after injection, likely due to extra-renal toxicity. We also found that haploinsufficient mice (*Prkdc*^{+/-}) developed a milder form of ADR nephropathy within 14–21 days of ADR administration (*P* < 0.05, *t* test, compared with *Prkdc*^{-/-} mice), developing glomerular mesangial sclerosis, cystic tubular dilatation, and proteinaceous casts (Figure 2, D–F). Finally, this milder phenotype was never observed in (B6 × BALB) F₁ hybrids (Figure 2, A–C), indicating that the R2140 mutation in BALB mice is not a complete loss of function. In contrast, the presence of 2 *Prkdc*^{BALB} alleles in (BALB × B6) F₂ mice resulted in ADR nephropathy (Figure 2J). These data demonstrated a gene-dosage effect in the development of ADR nephropathy.

PRKDC is expressed in podocytes, and its overexpression protects podocytes from ADR cytotoxicity. As podocytes are the site of primary damage in ADR nephropathy (1, 2), we further verified that PRKDC is expressed in these cells using immunohistochemistry and con-

firmed that PRKDC expression in the glomerulus was restricted to endothelial cells and podocytes with a nuclear localization pattern (Figure 3, A and B). To further examine the role of PRKDC in ADR resistance in podocytes, we generated a mouse podocyte clone (*Prkdc*⁺) stably overexpressing *Prkdc* at approximately 10-fold higher levels, compared with the control podocyte cell line (Figure 3C). We next compared podocyte survival in both lines at 7 days after ADR exposure at 2 concentrations (0.1 and 0.2 μg/ml). To identify the possible induction of cell proliferation by *Prkdc* overexpression, we monitored cell morphology and confluence after ADR exposure, as podocytes have very distinct cell morphology in differentiated and proliferating states. In control podocytes harboring the B6 *Prkdc* allele, ADR produced a dose-dependent decrease in cell number, with no areas of proliferation or visible changes in cell morphology, resulting in less than 25% cell survival after exposure (*t* test, *P* < 0.005). On the other hand, overexpression of *Prkdc* resulted in near-complete survival of podocytes (Figure 3D), without evidence of proliferation, suggesting that the enhanced survival was due to decreased apoptosis. The localization of PRKDC to podocytes is consistent with the known pathogenesis of ADR nephropathy, and the rescue of cytotoxicity by its overexpression provides further proof that *Prkdc* protects against ADR-induced podocyte damage.

ADR induced significant depletion of kidney mtDNA in mice with the Prkdc susceptibility allele. ADR produces cytotoxic damage via a variety of mechanisms, such as DNA intercalation and topoisomerase inhibition, but mtDNA damage has been implicated as a major mechanism for toxicity in nonreplicating cells, such as cardiomyocytes (12, 21). We therefore examined mtDNA levels in renal tissue by quantitative PCR (qPCR) and Southern blot and compared the levels in ADR-treated mice carrying different *Prkdc* alleles (Figure 4, A and B). While baseline mtDNA levels were similar between the

**Figure 3**

PRKDC is expressed in podocytes, and its overexpression protects against ADR cytotoxicity. Immunohistochemistry of human kidney with PAS counterstain demonstrates expression of PRKDC (brown staining) in the nuclei of podocytes (short arrows) and endothelial cells (arrowhead) of the glomerulus. The glomerular basement membrane (GBM [long arrow, magenta]) and Bowman's capsule landmarks allow identification of podocytes by their anatomic location, as podocytes are the only glomerular cell type overlying the glomerular basement membrane in the urinary space (outside the glomerular capillaries). Original magnification, $\times 600$ (A); $\times 1,000$ (B). (C) The Western blot shows an increased level of Prkdc in murine podocyte clone stably overexpressing Prkdc (Prkdc⁺) as compared with that of control podocytes. The positions of Prkdc and Gapdh (loading control) are indicated by arrows. (D) Comparison of survival among control and overexpressing Prkdc (Prkdc⁺) podocytes after treatment with 0.1 and 0.2 $\mu\text{g/ml}$ ADR. The ADR-treated groups were compared with the untreated control within each cell type.

sensitive and resistant strains, ADR administration resulted in 2.3-fold mtDNA depletion in F₂ mice homozygous for the *Prkdc* susceptibility allele, which developed nephropathy within 14 days of ADR administration (*t* test, $P = 0.003$; Figure 4A). This mtDNA depletion detected by qPCR was further confirmed by Southern blot analysis of the same DNA samples (Figure 4B). Time-course analyses demonstrated that by 14 days after treatment, ADR induced a 1.7-fold increase in mtDNA in B6 mice (*t* test $P < 0.05$) but a significant 1.9-fold reduction in BALB mice (*t* test, $P < 0.03$), resulting in approximately 3-fold difference between the strains (*t* test, $P = 0.008$; Figure 4C). These findings were further confirmed by the correlated changes in Tfam, a mtDNA-binding protein whose expression normally parallels mtDNA levels (Figure 4D). These data therefore raised the possibility that Prkdc participates in mtDNA maintenance, perhaps via a direct function in mitochondria. However, confocal microscopy of podocytes and 293 HEK cells demonstrated nuclear localization of PRKDC, and there was no evidence of colocalizations with mitochondrial markers (Mitotraker Red) in control conditions or after ADR treatment (Figure 4, E–G, and Supplemental Figure 3, A–F). We also did not detect PRKDC in proteinase K–treated mitochondrial fractions isolated from the kidney (Supplemental Figure 3J). These findings suggest indirect involvement of Prkdc in mtDNA maintenance, likely through intermediate proteins in the pathway.

Genetic interaction between Prkdc and Mpv17 provides evidence for participation of Prkdc in mtDNA maintenance. The mtDNA depletion in ADR nephropathy resembles the phenotype of patients with MDDS, a heterogeneous group of disorders produced by impairment in mtDNA synthesis or mitochondrial deoxynucleotide metabolism (28). In particular, mutations in some MDDS genes, such as *Mpv17*, encoding a mitochondrial inner membrane protein, predominantly manifest as nephropathy in mice (26, 30). *Mpv17*-null mice only manifest late-onset kidney disease due to glomerular mtDNA depletion (age > 200 days), suggestive of an indolent form of ADR nephropathy. Considering that *Prkdc* and *Mpv17* are expressed in the nuclear and mitochondrial compart-

ments, respectively, and deficiency of either gene alone does not produce overt organ dysfunction at an early age regardless of genetic background (30, 36, 37, 39, 40), tests of genetic interaction between these genes would provide compelling evidence for primary participation of Prkdc in mtDNA maintenance. Accordingly, we generated a cross between B6.CB17 (harboring the *Prkdc*^{SCID} allele) and *Mpv17*-null strains to determine the effect of reducing *Prkdc* gene dosage on mtDNA levels. While mice homozygous for *Prkdc* or *Mpv17* mutation alone showed no overt cardiac, hepatic, or renal lesions and longevity up to 12 months of age, loss of *Prkdc* gene dosage in *Mpv17*^{-/-} mice resulted in spontaneous and early-onset kidney, liver, and heart disease, resulting in significant mortality by 16 weeks of age (log-rank test, $P = 1 \times 10^{-4}$; Figure 5). The double homozygote mutants had the worst outcome, including significantly lower survival compared with mice with that of *Prkdc*-haploinsufficient mice (log-rank test, $P < 1 \times 10^{-3}$), and 23% manifested severe ascites at demise (Figure 5A and Supplemental Figure 4A). Histopathologic examination demonstrated glomerulosclerosis, cystic tubular dilatation, and proteinaceous casts in the kidney (Figure 5C) and hepatocyte nuclear enlargement, apoptosis, cytoplasmic vacuolization, congestion, and necrosis in the liver (Figure 5D and Supplemental Figure 4, B–D). In addition, we noted myocyte atrophy, fibrosis, and inflammation in the heart (Figure 5E). Electron microscopy studies in cardiac tissue showed significant loss of mitochondrial architecture in double-null *Prkdc*^{SCID/SCID}*Mpv17*^{-/-} mice, compared with that of *Prkdc*^{+/+}*Mpv17*^{-/-} mice (Figure 5, F and G, and Supplemental Figure 4, E and F). We next measured mtDNA levels in all 3 tissues using qPCR and evaluated the effects of *Prkdc* gene deletion in *Mpv17*-null mice (Figure 5B). We found a linear decrease in mtDNA level with decreasing *Prkdc* gene dosage in the kidney and heart, particularly in double-mutant mice compared with the groups with the wild-type *Prkdc* allele. Consistent with previous reports of *Mpv17*-null mice, there was severe mtDNA depletion in livers of all 3 groups ($< 10\%$ of control) and only a trend toward worse depletion in double-mutant mice. The severe mtDNA depletion detected in the liver may be explained

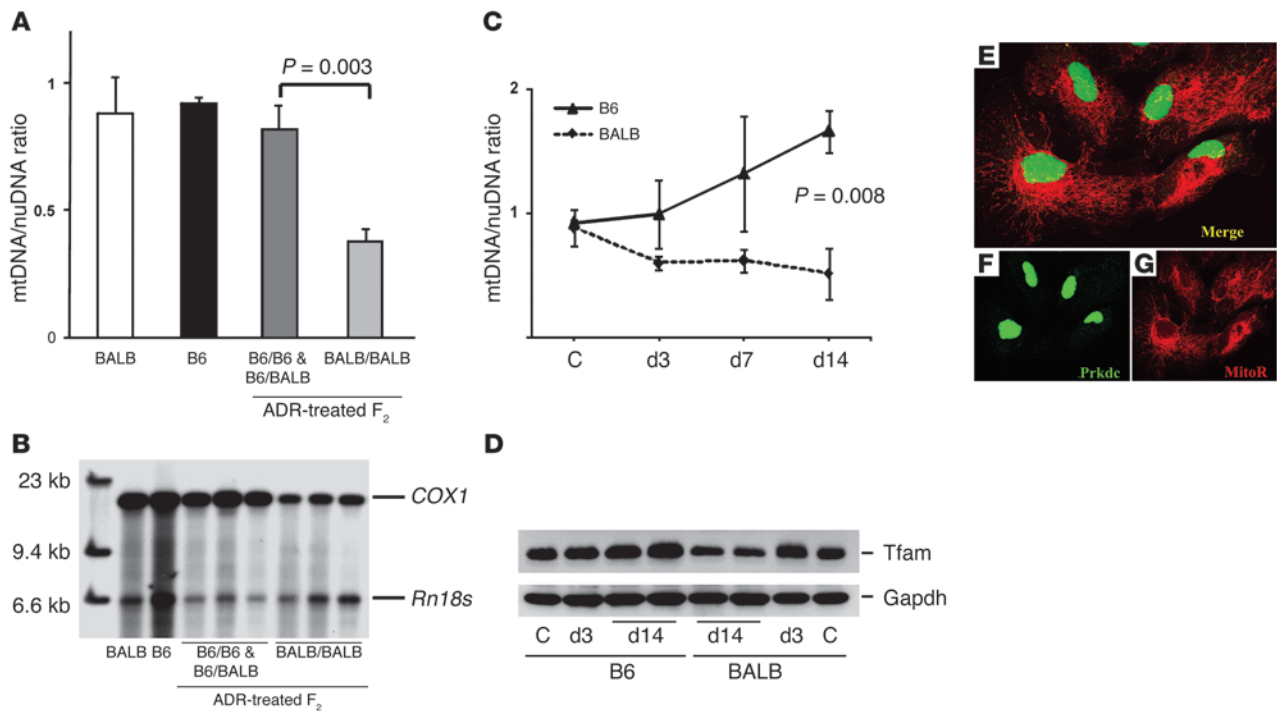


Figure 4 mtDNA depletion in ADR nephropathy. **(A)** qPCR analysis of kidney mtDNA levels demonstrates mtDNA depletion at day 14 after ADR treatment in (BALB × B6) F₂ mice homozygous for the susceptibility alleles at the *Prkdc* locus (BALB/BALB mice, *n* = 8), compared with those of mice with the BALB/B6 or B6/B6 genotypes (*n* = 6). mtDNA levels are presented as a mtDNA/nuDNA ratio, calculated for the mitochondria-encoded *COX1* and nuclear-encoded *Rn18s* genes, standardized to the B6 control sample. **(B)** Southern blot of total kidney DNA from parental strains and representative ADR-treated (B6 × BALB) F₂ mice shown in **A**. The positions of *COX1* and *Rn18s* genes are indicated by bars, and the *Prkdc* genotypes are indicated. **(C)** Time-course analysis (qPCR) of mtDNA levels in ADR-treated mice shows marked mtDNA depletion by 14 days in BALB mice (*n* = 3 per strain at each time point). C, control. **(D)** The Western blot shows ADR-induced changes in Tfam levels, which corresponded to changes in mtDNA levels in **C**. **(E–G)** Confocal microscopy of podocytes demonstrates that Prkdc (green staining) is localized to the nucleus but is not colocalized with a mitochondria marker (Mitotraker red [MitoR]). Original magnification: 230 × 230 microns (**E–G**).

by the very low baseline level of Prkdc in the liver (Supplemental Figure 1), which suggests that all 3 groups can be considered as “liver-specific” double mutants from a functional point of view.

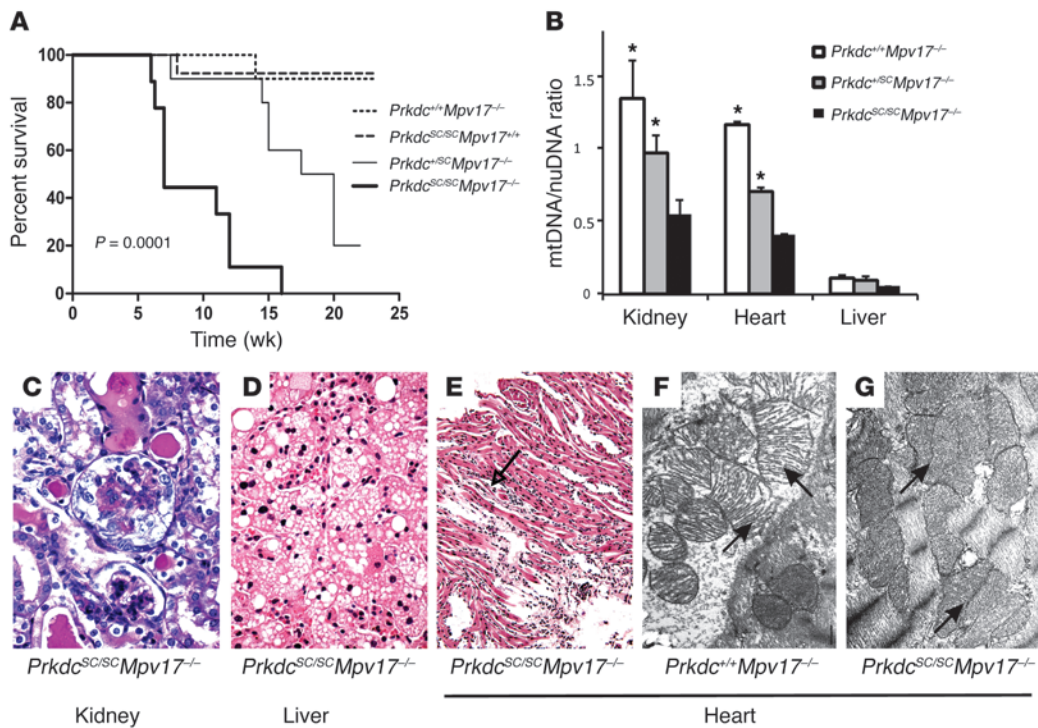
The findings of spontaneous heart, liver, and kidney lesions and mtDNA depletion in double homozygote mice provide strong evidence of genetic interaction between *Prkdc* and *Mpv17*, as neither *Mpv17*- nor *Prkdc*-null mice, described on different genetic backgrounds, have these severe early clinical phenotypes (30, 36, 37, 39, 40). Nevertheless, to further rule out a genetic background effect, we performed a genome-wide scan, with 732 informative markers in the *Prkdc/Mpv17* cross. Analysis of linkage found significant linkage of cardiac and renal mtDNA levels, but not of liver mtDNA levels, to the *Prkdc* locus on chromosome 16A1 (lod scores of 4.6 and 3.2, respectively; Supplemental Figure 5). There were no other loci across the genome that explained variation in these traits. This analysis ruled out a genetic background effect on our phenotypes and further implicated genetic interaction between *Prkdc* and *Mpv17* as the cause of synthetic pathology.

Discussion

This study identifies a mutation in *Prkdc* as the genetic basis of interstrain susceptibility to murine ADR nephropathy, one of the most commonly used experimental models of kidney injury. Our findings are supported by precise mapping data, identification of

a nonconservative missense variant with loss of protein expression in susceptible strains, and recapitulation of ADR nephropathy in 2 strains, with independent mutations in *Prkdc*. We also showed that Prkdc is expressed in podocytes, the principal cell injured in ADR nephropathy, and its overexpression in podocytes cell lines results in increased survival after ADR treatment. We further found that ADR nephropathy produces significant mtDNA depletion in mice homozygous for mutant *Prkdc* alleles, suggesting what we believe to be a novel role for Prkdc in mtDNA maintenance. This was confirmed by our studies of the genetic interaction of *Prkdc* with the *Mpv17*, a gene that is expressed in mitochondria and is mutated in human MDDS. The finding of spontaneous mtDNA depletion in *Prkdc/Mpv17* double-mutant mice simultaneously implicates mtDNA damage in the pathogenesis of ADR nephropathy and to our knowledge, identifies *Prkdc* as novel component of the mitochondrial genome maintenance pathway.

Prkdc encodes the catalytic subunit of the trimeric DNA-dependent protein kinase (DNA-PKcs) and has essential roles in DNA repair, signal transduction, and transcriptional activation. Genetic defects in the *Prkdc* or the *Ku70* and *Ku80* genes (encoding the regulatory subunits of DNA-PK) result in immunodeficiency, radiosensitivity, and premature aging, which are generally attributed to the requirement for DNA-PK in nonhomologous end-joining DSB repair, the primary mode of DNA repair in nonreplicating cells (34, 38, 41).

**Figure 5**

An intercross between *Mpv17*^{-/-} and *Prkdc*^{SCID/SCID} mice confirms genetic interaction between *Mpv17* and *Prkdc*. (A) Kaplan-Meier survival analysis demonstrates that decreasing *Prkdc* gene dosage markedly reduces survival in *Mpv17*-null mice ($n = 8-18$ mice per group; log-rank test, $P = 0.0001$). (B) Association between *Prkdc* genotype and mtDNA depletion in tissues of *Mpv17*-null mice ($*P < 0.05$, t test, compared with the *Mpv17*^{-/-}*Prkdc*^{SCID/SCID} group). (C-E) Histopathology demonstrates the development of glomerulosclerosis and tubulointerstitial damage, with cast formation in the kidney (C); hepatocyte nuclear enlargement, ballooning cytoplasmic vacuolization, and sinusoidal congestion in the liver (D); and myocyte atrophy (arrow), fibrosis, and inflammation in the heart of double-mutant mice (E). (F and G) Electron microscopy of heart tissue shows structural lesions in the mitochondria of double-null mice (G) as compared with *Mpv17*-null mice (F). Mitochondria are indicated by arrows. Original magnification: $\times 600$ (C and D); $\times 200$ (E); $\times 30,000$ (F and G). SC, the SCID allele.

Upon initiation of DSBs, *Prkdc* is recruited by the Ku70 and Ku80 subunits and aligns broken DNA ends, enabling DNA polymerase and other ligation factors to repair the breaks (34, 38, 41). This DSB repair function is also essential in lymphocyte development, which necessitates repeated rounds of DNA break and repair during VDJ recombination (42). *Prkdc* also participates in signal transduction cascades related to apoptotic cell death (43), telomere maintenance, and genome surveillance (44). Most recently, *Prkdc* has also been implicated as an essential coactivator of multiple transcription factors (45). In this function, *Prkdc* is part of a multimeric protein complex that unwinds DNA through site-specific induction and repair of DSBs, thereby facilitating access of transcription factors to their binding sites. To date, the *Prkdc* containing complex has been implicated in coactivation of the estrogen receptor, USF (46), Sp1 (47) NRF1 (48), or FoxA2 (49). Moreover, *Prkdc*-deficient cells manifest global defects in transcriptional activation, suggesting that *Prkdc* regulates many additional transcription factors and metabolic processes (50). Interestingly, there may be critical thresholds for completion of multifaceted functions of *Prkdc*. For example, BALB mice produce a very low level of *Prkdc* protein, which is functionally sufficient for lymphocyte maturation but insufficient to resist DNA-damaging agents, such as ADR. More deleterious *Prkdc* mutations, such as the SCID mutation or complete null alleles, result in immunodeficiency, radiosensitivity, and premature aging (38). Consistent with these findings, the severity of response to ADR var-

ied according to functional deficit in *Prkdc* alleles: null mice demonstrated early lethality and susceptibility to ADR nephropathy; the near-null SCID mice displayed ADR nephropathy but survived longer; and haploinsufficient mice developed a milder form of ADR nephropathy within 14–21 days of ADR administration, which was never observed in (B6 \times BALB) F₁ hybrids.

Here, we identify what we believe to be a novel role for *Prkdc* in maintenance of the mitochondrial genome. We detected significant kidney mtDNA depletion in ADR-treated mice homozygous for *Prkdc* susceptibility alleles, consistent with data demonstrating that mtDNA depletion is the major mechanism of ADR injury in postmitotic cells, likely due to direct intercalation into mtDNA (51). However, we did not detect colocalization of PRKDC with mitochondrial markers in podocytes or 293HEK cells or in proteinase K-treated kidney mitochondrial fractions, suggesting that it did not contribute to mtDNA maintenance via a direct function within mitochondria. Since *Prkdc* has many roles in signal transduction and transcriptional regulation, the alternative hypothesis was that it participates in a nuclear signaling pathway that sustains the integrity of mtDNA or promotes mitochondrial biogenesis subsequent to genotoxic stress. This hypothesis was consistent with the results of a recent RNAi screen, showing that genes required for ADR resistance in yeast are involved in nuclear DNA repair as well as mitochondrial homeostasis, demonstrating a link between these pathways (52).



To confirm that *Prkdc* participates in mtDNA maintenance, we performed tests of genetic interaction between *Prkdc* and *Mpv17* genes. The *Mpv17* gene was an excellent candidate for testing genetic interaction because it encodes a mitochondrial inner membrane protein and its mutations produce MDDS in humans and mice (26, 30). Moreover, *Mpv17* mutant mice do not manifest early-onset organ dysfunction, providing an unambiguous starting point for testing the effect of *Prkdc* gene dosage on phenotype (26, 30). While mice with mutations in either single gene were asymptomatic up to 12 months of age, *Prkdc/Mpv17* double-mutant mice developed significant cardiac and renal mtDNA depletion and spontaneous liver, heart, and kidney disease, resulting in excess mortality by 16 weeks of age. The double-mutant mice also displayed severe mitochondrial structural lesions in cardiomyocytes by electron microscopy. These findings recapitulated both MDDS and ADR injury phenotypes in the absence of ADR, demonstrating that the 2 mutations introduced genetic lesions in a common pathway critical to mtDNA maintenance.

It is difficult to predict the precise molecular mechanism through which *Prkdc* regulates mtDNA, because we still have a limited knowledge of the nuclear-mitochondrial communication pathways mediating mtDNA maintenance. The known MDDS genes do not account for all the cases, and the function of some genes, such as *Mpv17*, remains largely unknown, suggesting many yet-undiscovered components of this pathway. Since *Prkdc* is a multifunctional protein, it may regulate *MPV17* or any of genes implicated in MDDS via one of its described functions: as a kinase, as a signal transduction protein, or as a transcriptional coactivator. Alternatively, *Prkdc* may participate in an “emergency” mtDNA maintenance pathway, which is dormant under normal conditions but is activated in DNA-damaging conditions. In this regard, *Prkdc* was recently found to participate in coactivation of *NRF1*, a transcription factor critical for mitochondrial biogenesis (48), and, thus, one can hypothesize that *Prkdc* mutations prevent an adequate biogenic response to genotoxic stress. These hypotheses form plausible starting points for future investigation, but given the manifold functions of *Prkdc*, we expect that a broad array of experiments will be required to adequately dissect its exact role in the mtDNA maintenance pathway.

Mutations in genes that are ubiquitously expressed can result in cell- and organ-specific defects, but the underlying reasons for this are frequently not understood. For example, the *ACTN4*, *IFN2*, or *TRPC6* genes are broadly expressed, but their mutations produce podocyte dysfunction and nephropathy (53–55). Similarly, mutations in some genes encoding mitochondrial respiratory chains produce podocyte dysfunction, while acquired mtDNA mutations have also been described in focal segmental glomerulosclerosis lesions (56, 57). One can surmise that genetic mutations produce functional defects only in cells/organs lacking redundant or modifier pathways or in the setting of specific physiologic states or metabolic demands. In the case of podocytes, we can also hypothesize that their terminally differentiated state would prevent cell division and limit repair subsequent to injury. Our study provides additional insight into the problem of variable organ injury in MDDS. We identify *Prkdc* and its downstream pathways as logical candidate modifiers that may explain variable severity of mtDNA depletion, disease onset, and target organ damage in MDDS patients and mouse models. Finally, the finding of cardiac mtDNA depletion and cardiomyopathy in the *Prkdc/Mpv17* double-mutant mice is also very intriguing, because cardiotoxicity due to mtDNA

depletion is the main side effect of ADR therapy in humans. These findings suggest that elucidation of the components of the PRKDC/MPV17 signaling pathway may inform about biological mechanisms mediating ADR-mediated cardiomyopathy.

Recent data have also implicated 2 *Prkdc* homologs (*ATM* and *ATL-1*) in regulation of mtDNA levels in mammalian and worm cells (58, 59). Ataxia-telangiectasia mutated (*ATM*), another PI3K involved in the homologous recombination DSB repair, has been shown to participate in mitochondrial genome maintenance via regulation of the RRM2B subunit of ribonucleotide reductase, which is critical for de novo generation of deoxynucleotides and is mutated in some patients with MDDS (27, 58, 60). The *ATM*-mediated RRM2B regulation thus presents a strong parallel to the *Prkdc/Mpv17* interaction observed in the present study, offering another link between the PI3K gene family and the MDDS pathway. Similarly, inactivation of *ATL-1* causes significant mtDNA loss in *Caenorhabditis elegans*, but downstream pathways have not been identified. Together with our study, these data indicate a new general pathway linking the nuclear DNA repair program to mtDNA regulation. Identification of additional components of this novel nuclear-mitochondrial communication pathway may uncover alternative mechanisms of mtDNA maintenance and further elucidate pathways underlying organ dysfunction in MDDS or anthracycline-mediated toxicity.

Methods

Mice. Inbred strains, *Mpv17*-null mice, and B6.CB17-*Prkdc^{scid}/SzJ* (B6.CB17) mice were purchased from The Jackson Laboratory. *Mpv17*-null mice were bred onto an FVB/NJ genetic background for more than 10 generations. *Prkdc*-knockout mice on the B6 background were a gift from D. Chen (University of Texas Southwestern Medical Center, Dallas, Texas, USA) (37). To refine the ADR nephropathy susceptibility locus, we produced 176 F₂ and 1,446 backcross progeny between BALB and B6 mice and phenotyped 68 mice with informative recombinations between rs4164770 and rs4165049. ADR nephropathy was produced by tail vein injection (10 mg/kg) (31). Heterozygous (*Prkdc^{+/−}*) and homozygous (*Prkdc^{−/−}*) *Prkdc*-knockout mice and control BALB × B6-F₁ hybrid mice were injected with ADR, as above, at 16 to 20 weeks of age. For a time-course analysis, BALB and B6 mice were injected with ADR, as above (in triplicates for each strain), and sacrificed at 3 hours and 3, 7, and 14 days after injection. To assess the phenotypic effect of combination of mutant *Prkdc* and *Mpv17* alleles, we generated an intercross between B6.CB17 (SCID) and *Mpv17*-null strain ($n = 152$) and analyzed the effect of *Prkdc* gene dosage on a *Mpv17*-null background. These mice were followed up to 23 weeks, and kidneys, hearts, and livers were collected at sacrifice. The protocol was approved by the IACUC at the Columbia University Medical Center.

Genotyping, sequencing, and quantitative analysis of mtDNA. Microsatellite markers were genotyped by capillary electrophoresis. SNP loci for inbred strains were obtained from NCBI and the Mouse Phenome Database (<http://phenome.jax.org/>), and additional SNP loci were genotyped by direct sequencing. Total kidney DNA was isolated using the DNeasy Tissue Kit (Qiagen). mtDNA levels were quantitated by qPCR using SYBR Green Mix (Bio-Rad) and presented as a ratio of mitochondria-encoded *COX1* to nuclear-encoded *Rn18s*, standardized to a reference sample (B6) included in each run. The *COX1* and *Rn18s* probes for Southern blotting were generated using the PCR DIG Probe Synthesis Kit (Roche). Total DNA was digested with *SacI* enzyme, separated, transferred onto nylon membrane, and hybridized with the probes, and the membrane was developed using anti-DIG-AP antibody (Roche). The primer sequences are listed in Supplemental Table 1. To exclude a genetic background effect, we performed a genome scan in the *Mpv17/SCID* cross, using the Illumina Mouse Medium Density Set. In this



genotyping set, 732 SNP loci were informative between FVB and B6. Analysis of linkage of mtDNA levels was performed using the Haley-Knott regression method and the R/QTL program (<http://www.rqtl.org>). LOD scores of more than 3 were considered significant.

Western blot. Western blot analysis of whole kidney lysates (100 µg of total protein per well) was performed using the Immobilon Western ECL Detection Kit (Millipore) and the following antibodies: monoclonal mouse anti-DNA-PKcs Ab-4 (Neomarkers), anti-GAPDH (R&D Systems), goat mt-TFA (A-17) antibody (Santa Cruz Biotechnology Inc.), HRP-labeled sheep anti-mouse antibody (Amersham), and donkey anti-goat antibody (Santa Cruz Biotechnology Inc.).

Cell culture. Conditionally immortalized murine and human podocyte cells were gifts from P. Klotman (Mount Sinai Hospital, New York, New York, USA) and J. Reiser. The murine podocyte cells (MPCs) harbored the B6 haplotype at the *Prkdc* locus. A murine clone stably overexpressing *Prkdc* (*Prkdc*⁺) was selected after transfection with the EF-*Prkdc*.pGEM 9 plasmid, which encoded the full-length cDNA of mouse *Prkdc* from B6 mice under elongation factor α (EF) promoter and zeocin resistance cassette. Podocytes were differentiated for 14 days at 37°C prior to experiments. MPCs were treated with 0.1 or 0.2 µg/ml ADR for 24 hours, and then the medium was changed and incubation was continued for 7 days, at which point the cells were collected and counted for survival analysis.

Immunohistochemistry and confocal microscopy. Kidneys, hearts, and livers were formalin fixed and paraffin embedded, and 3-µm sections were cut and stained with H&E or periodic acid-Schiff (PAS) or used for immunohistochemistry. The total histologic kidney injury score was calculated as an average of 4 histologic scores (acute tubular injury, tubular cast dilatation, mesangial sclerosis, and glomerulosclerosis scores), quantified on the 0–3+ scale. Immunohistochemistry was performed using mouse monoclonal antibody DNA-PKcs Ab-4 (Neomarkers) and HRP-labeled goat anti-mouse DakoCytomation EnVision+ system (Dako), followed by diaminobenzidine. The glomerular basement membrane was visualized with PAS reaction, without a nuclear counterstain. The podocytes were

localized specifically by their anatomic location, as they are the only glomerular cell type overlying the glomerular basement membrane in the urinary space (outside the glomerular capillaries).

For confocal microscopy, differentiated human podocytes or 293HEK cells were incubated with Mitotraker Red (Invitrogen), fixed with 4% paraformaldehyde, and stained with mouse DNA-PKcs Ab-4 (Neomarkers) and goat anti-mouse Amaxa 488 antibody (Invitrogen). Control and ADR-treated (0.5 µg/ml) podocytes were compared in order to detect possible translocation of Prkdc to the mitochondria in stress conditions.

Statistics. Comparisons of mtDNA among strains were performed by 2-sided *t* tests. Data represent mean \pm SEM. Survival analysis in *Prkdc*/*Mpv17* intercross mice was performed using Kaplan-Meier analysis and log-rank (Mantel-Cox) test, with a global comparison between genotype groups, and by comparisons of groups with the ≥ 3 mutant alleles to groups with single-gene mutant homozygotes. *P* values of less than 0.05 were considered significant.

Acknowledgments

We thank Estela Area-Gomez for help with mitochondria methodology and Richard Lifton, Michio Hirano, and our laboratory members for insightful discussions. A.G. Gharavi is supported by the Columbia Center for Glomerular Diseases. This study was also supported by the histology core facility of the Columbia Diabetes and Endocrinology Research Center (NIH P30-DK63608).

Received for publication May 17, 2010, and accepted in revised form August 25, 2010.

Address correspondence to: Ali G. Gharavi, Department of Medicine, Columbia University College of Physicians and Surgeons, 1150 St. Nicholas Ave., Russ Berrie Pavilion 302, New York, New York 10032, USA. Phone: 212.851.5556; Fax: 212.305.5520; E-mail: ag2239@columbia.edu.

- Rossmann P, Matousovic K, Bohdanecka M. Experimental adriamycin nephropathy. Fine structure, morphometry, glomerular polyanion, and cell membrane antigens. *J Pathol.* 1993;169(1):99–108.
- Wang Y, Wang YP, Tay YC, Harris DC. Progressive adriamycin nephropathy in mice: sequence of histologic and immunohistochemical events. *Kidney Int.* 2000;58(4):1797–1804.
- Kaplan BS, Renaud L, Drummond KN. Effects of aminonucleoside, daunomycin, and adriamycin on carbon oxidation by glomeruli. *Lab Invest.* 1976;34(2):174–178.
- Tryggvason K, Patrakka J, Wartiovaara J. Hereditary proteinuria syndromes and mechanisms of proteinuria. *N Engl J Med.* 2006;354(13):1387–1401.
- Kim YH, et al. Podocyte depletion and glomerulosclerosis have a direct relationship in the PAN-treated rat. *Kidney Int.* 2001;60(3):957–968.
- Wharram BL, et al. Podocyte depletion causes glomerulosclerosis: diphtheria toxin-induced podocyte depletion in rats expressing human diphtheria toxin receptor transgene. *J Am Soc Nephrol.* 2005;16(10):2941–2952.
- Wiggins JE, et al. Podocyte hypertrophy, “adaptation,” and “decompensation” associated with glomerular enlargement and glomerulosclerosis in the aging rat: prevention by calorie restriction. *J Am Soc Nephrol.* 2005;16(10):2953–2966.
- Bertani T, et al. Adriamycin-induced nephrotic syndrome in rats: sequence of pathologic events. *Lab Invest.* 1982;46(1):16–23.
- Cao Q, et al. IL-10/TGF- β -modified macrophages induce regulatory T cells and protect against adriamycin nephrosis. *J Am Soc Nephrol.* 2010;21(6):933–942.
- Cheng H, Fan X, Guan Y, Moeckel GW, Zent R, Harris RC. Distinct roles for basal and induced COX-2 in podocyte injury. *J Am Soc Nephrol.* 2009;20(9):1953–1962.
- Dai C, Stolz DB, Kiss LP, Monga SP, Holzman LB, Liu Y. Wnt/ β -catenin signaling promotes podocyte dysfunction and albuminuria. *J Am Soc Nephrol.* 2009;20(9):1997–2008.
- Grenier MA, Lipshultz SE. Epidemiology of anthracycline cardiotoxicity in children and adults. *Semin Oncol.* 1998;25(4 suppl 10):72–85.
- Fukuda F, Kitada M, Horie T, Awazu S. Evaluation of adriamycin-induced lipid peroxidation. *Biochem Pharmacol.* 1992;44(4):755–760.
- Paczek L, Teschner M, Schaefer RM, Kovar J, Romen W, Heidland A. Intraglomerular proteinase activity in adriamycin-induced nephropathy. *Nephron.* 1992;60(1):81–86.
- Coers W, Huitema S, van der Horst ML, Weening JJ. Puromycin aminonucleoside and adriamycin disturb cytoskeletal and extracellular matrix protein organization, but not protein synthesis of cultured glomerular epithelial cells. *Exp Nephrol.* 1994;2(1):40–50.
- Akman SA, Doroshov JH, Burke TG, Dizdaroglu M. DNA base modifications induced in isolated human chromatin by NADH dehydrogenase-catalyzed reduction of doxorubicin. *Biochemistry.* 1992;31(13):3500–3506.
- Tewey KM, Rowe TC, Yang L, Halligan BD, Liu LF. Adriamycin-induced DNA damage mediated by mammalian DNA topoisomerase II. *Science.* 1984;226(4673):466–468.
- Lawrence JW, Darkin-Rattray S, Xie F, Neims AH, Rowe TC. 4-Quinolones cause a selective loss of mitochondrial DNA from mouse L1210 leukemia cells. *J Cell Biochem.* 1993;51(2):165–174.
- Adachi K, et al. A deletion of mitochondrial DNA in murine doxorubicin-induced cardiotoxicity. *Biochem Biophys Res Commun.* 1993;195(2):945–951.
- Lebrecht D, Kokkari A, Ketelsen UP, Setzer B, Walker UA. Tissue-specific mtDNA lesions and radical-associated mitochondrial dysfunction in human hearts exposed to doxorubicin. *J Pathol.* 2005;207(4):436–444.
- Suliman HB, Carraway MS, Ali AS, Reynolds CM, Welty-Wolf KE, Piantadosi CA. The CO/HO system reverses inhibition of mitochondrial biogenesis and prevents murine doxorubicin cardiomyopathy. *J Clin Invest.* 2007;117(12):3730–3741.
- Gross NJ, Getz GS, Rabinowitz M. Apparent turnover of mitochondrial deoxyribonucleic acid and mitochondrial phospholipids in the tissues of the rat. *J Biol Chem.* 1969;244(6):1552–1562.
- Palmeira CM, Serrano J, Kuehl DW, Wallace KB. Preferential oxidation of cardiac mitochondrial DNA following acute intoxication with doxorubicin. *Biochim Biophys Acta.* 1997;1321(2):101–106.
- Cannino G, Di Liegro CM, Rinaldi AM. Nuclear-mitochondrial interaction. *Mitochondrion.* 2007;7(6):359–366.
- Scarpulla RC. Transcriptional paradigms in mammalian mitochondrial biogenesis and function. *Physiol Rev.* 2008;88(2):611–638.
- Spinazzola A, et al. MPV17 encodes an inner mitochondrial membrane protein and is mutated in infantile hepatic mitochondrial DNA depletion.



Nat Genet. 2006;38(5):570–575.

27. Bourdon A, et al. Mutation of RRM2B, encoding p53-controlled ribonucleotide reductase (p53R2), causes severe mitochondrial DNA depletion. *Nat Genet.* 2007;39(6):776–780.

28. Rahman S, Poulton J. Diagnosis of mitochondrial DNA depletion syndromes. *Arch Dis Child.* 2009;94(1):3–5.

29. Kimura T, Takeda S, Sagiya Y, Gotoh M, Nakamura Y, Arakawa H. Impaired function of p53R2 in Rrm2b-null mice causes severe renal failure through attenuation of dNTP pools. *Nat Genet.* 2003;34(4):440–445.

30. Viscomi C, et al. Early-onset liver mtDNA depletion and late-onset proteinuric nephropathy in Mpv17 knockout mice. *Hum Mol Genet.* 2009;18(1):12–26.

31. Zheng Z, et al. A Mendelian locus on chromosome 16 determines susceptibility to doxorubicin nephropathy in the mouse. *Proc Natl Acad Sci U S A.* 2005;102(7):2502–2507.

32. Zheng Z, Pavlidis P, Chua S, D'Agati VD, Gharavi AG. An ancestral haplotype defines susceptibility to doxorubicin nephropathy in the laboratory mouse. *J Am Soc Nephrol.* 2006;17(7):1796–1800.

33. Mott R. A haplotype map for the laboratory mouse. *Nat Genet.* 2007;39(9):1054–1056.

34. Dip R, Naegeli H. More than just strand breaks: the recognition of structural DNA discontinuities by DNA-dependent protein kinase catalytic subunit. *FASEB J.* 2005;19(7):704–715.

35. Staub E, Fiziev P, Rosenthal A, Hinzmann B. Insights into the evolution of the nucleolus by an analysis of its protein domain repertoire. *Bioessays.* 2004;26(5):567–581.

36. Blunt T, et al. Defective DNA-dependent protein kinase activity is linked to V(D)J recombination and DNA repair defects associated with the murine scid mutation. *Cell.* 1995;80(5):813–823.

37. Kurimasa A, et al. Catalytic subunit of DNA-dependent protein kinase: impact on lymphocyte development and tumorigenesis. *Proc Natl Acad Sci U S A.* 1999;96(4):1403–1408.

38. Araki R, et al. Nonsense mutation at Tyr-4046 in the DNA-dependent protein kinase catalytic subunit of severe combined immune deficiency mice. *Proc Natl Acad Sci U S A.* 1997;94(6):2438–2443.

39. O'Bryan T, Weiher H, Rennke HG, Kren S, Hostetter TH. Course of renal injury in the Mpv17-deficient transgenic mouse. *J Am Soc Nephrol.* 2000;11(6):1067–1074.

40. Jhappan C, Morse HC 3rd, Fleischmann RD, Gottesman MM, Merlino G. DNA-PKcs: a T-cell tumour suppressor encoded at the mouse scid locus. *Nat Genet.* 1997;17(4):483–486.

41. O'Driscoll M, Jeggo PA. The role of double-strand break repair - insights from human genetics. *Nat Rev Genet.* 2006;7(1):45–54.

42. Franco S, Murphy MM, Li G, Borjeson T, Boboila C, Alt FW. DNA-PKcs and Artemis function in the end-joining phase of immunoglobulin heavy chain class switch recombination. *J Exp Med.* 2008;205(3):557–564.

43. Burma S, et al. DNA-dependent protein kinase-independent activation of p53 in response to DNA damage. *J Biol Chem.* 1999;274(24):17139–17143.

44. d'Adda di Fagnana F, et al. Effects of DNA nonhomologous end-joining factors on telomere length and chromosomal stability in mammalian cells. *Curr Biol.* 2001;11(15):1192–1196.

45. Ju BG, et al. A topoisomerase IIbeta-mediated dsDNA break required for regulated transcription. *Science.* 2006;312(5781):1798–1802.

46. Wong RH, Chang I, Hudak CS, Hyun S, Kwan HY, Sul HS. A role of DNA-PK for the metabolic gene regulation in response to insulin. *Cell.* 2009;136(6):1056–1072.

47. Jackson S, Gottlieb T, Hartley K. Phosphorylation of transcription factor Sp1 by the DNA-dependent protein kinase. *Adv Second Messenger Phosphoprotein Res.* 1993;28:279–286.

48. Hossain MB, Ji P, Anish R, Jacobson RH, Takada S. Poly(ADP-ribose) Polymerase 1 Interacts with Nuclear Respiratory Factor 1 (NRF-1) and Plays a Role in NRF-1 Transcriptional Regulation. *J Biol Chem.* 2009;284(13):8621–8632.

49. Nock A, et al. Identification of DNA-dependent protein kinase as a cofactor for the forkhead transcription factor FoxA2. *J Biol Chem.* 2009;284(30):19915–19926.

50. Woodard RL, Anderson MG, Dynan WS. Nuclear extracts lacking DNA-dependent protein kinase are deficient in multiple round transcription. *J Biol Chem.* 1999;274(1):478–485.

51. Ashley N, Poulton J. Anticancer DNA intercalators cause p53-dependent mitochondrial DNA nucleoid re-modelling. *Oncogene.* 2009;28(44):3880–3891.

52. Xia L, Jaafar L, Cashikar A, Flores-Rozas H. Identification of genes required for protection from doxorubicin by a genome-wide screen in *Saccharomyces cerevisiae*. *Cancer Res.* 2007;67(23):11411–11418.

53. Kaplan JM, et al. Mutations in ACTN4, encoding alpha-actinin-4, cause familial focal segmental glomerulosclerosis. *Nat Genet.* 2000;24(3):251–256.

54. Winn MP, et al. A mutation in the TRPC6 cation channel causes familial focal segmental glomerulosclerosis. *Science.* 2005;308(5729):1801–1804.

55. Brown EJ, et al. Mutations in the formin gene INF2 cause focal segmental glomerulosclerosis. *Nat Genet.* 2010;42(1):72–76.

56. Rotig A, Munnich A. Genetic features of mitochondrial respiratory chain disorders. *J Am Soc Nephrol.* 2003;14(12):2995–3007.

57. Yamagata K, et al. Mitochondrial DNA mutations in focal segmental glomerulosclerosis lesions. *J Am Soc Nephrol.* 2002;13(7):1816–1823.

58. Eaton JS, Lin ZP, Sartorelli AC, Bonawitz ND, Shadel GS. Ataxia-telangiectasia mutated kinase regulates ribonucleotide reductase and mitochondrial homeostasis. *J Clin Invest.* 2007;117(9):2723–2734.

59. Mori C, Takanami T, Higashitani A. Maintenance of mitochondrial DNA by the *Caenorhabditis elegans* ATR checkpoint protein ATL-1. *Genetics.* 2008;180(1):681–686.

60. Chang L, et al. ATM-mediated serine 72 phosphorylation stabilizes ribonucleotide reductase small subunit p53R2 protein against MDM2 to DNA damage. *Proc Natl Acad Sci U S A.* 2008;105(47):18519–18524.